

MODELING OF COOKING AND COOLING PROCESSES OF TUNISIAN SALAMI

J. MEJRI^{*}, M.N. MELKI[†] and M. MEJRI[‡]

[†]Département Génie Mécanique et Agro-Industriel, Ecole Supérieure des Ingénieurs de Medjez el Bab, ESIM, 9070 Medjez el Bab, Tunisia

[‡]Unité de recherche: Les énergies renouvelables en agriculture et agro-industrie, Ecole Supérieure des Ingénieurs de Medjez el Bab, ESIM, 9070 Medjez el Bab, Tunisia

^{*}Corresponding author. Tel.: +216 97 577532; fax: + 216 78561700
E-mail address: jmejri2001@yahoo.fr

ABSTRACT

The aim of this paper is to develop and validate the heat transfer model in the cooking and cooling process of sausage products to analyze its effectiveness and performance. The modeling of the heat transfer was followed by a numerical simulation to predict the temperature evolution as a function of time. Solving the heat equation was carried out using the finite difference method. Discretizing the equation was carried out in space and in time. Then, a program developed on Matlab was used to solve the discrete equation. The cooked meat was in cylindrical shape ($D = 5.6 \text{ cm} \times L = 24 \text{ cm}$) and with a weight of $565 \text{ g} \pm 5 \text{ g}$. The predictions from the model are compared with the experimental results with good agreement ($R^2 = 0.98$ for cooking and $R^2 = 0.99$ for cooling process). The maximum deviation between measured and calculated temperatures was within 2.59°C for the cooking, within 1.49°C for the cooling by immersion water and within 0.19°C for the air cooling processes. Percentage differences between predicted and experimental temperatures for the cooking, cooling by immersion water and air cooling processes were around 1.58%, 1.72% and 0.66%, respectively. Thus, the developed model can be considered as a valuable tool to assess the effectiveness and the performance of cooking and cooling processes.

Keywords: cooked meat, salami, heat transfer, cooking, cooling, processes, modeling

1. INTRODUCTION

Thermal processing has remained the technology of choice to extend the shelf-life, to improve the eating quality and safety of food products. The meat industry is one of the most important food industries. In the cooked meat industry, rapid cooling is required to cool the meat after finishing the cooking process to safe storage temperature in order to minimize the growth of surviving microorganisms. Guidelines for the control of this cooling process for cooked meats have been issued and recommended by many European countries (SUN & WANG; 2006).

After removal from the cooking process, it is recommended that meat joints should be chilled from 74°C to 10°C within 2.5 h (SUN and WANG, 2006). If the meat products are cooled properly immediately after cooking, potential germination and outgrowth of spore-forming pathogenic microorganisms that are able to survive the heat treatment applied during cooking can be prevented.

In the last decade, a number of heat and mass transfer models for simulating cooling of ready-to-eat (RTE) meat products have been developed (CHEN *et al.*, 1999; HU and SUN, 2000; WANG and SUN, 2002a; DELGADO and SUN, 2003; WANG and SUN, 2004; AMÉZQUITA *et al.*, 2005; DRUMMOND and SUN, 2008; ; RINALDI *et al.*, 2011; CEPEDA *et al.*, 2013; COGNÉ *et al.*, 2013; KONDJAYAN *et al.*, 2013; RINALDI *et al.*, 2014; CHAPWANYA and MISRA, 2015).

However, existing models are subject to simplifications that limit their applicability in the meat industry. Some of the most common simplifications include (1) The process of slaughtering animals: ritual slaughter to which depends the obtained meat, (2) The microbiological quality of the meat used in the preparation of hams, (3) The operating parameters of the processing methods used in each country and (4) Consumption patterns of each population, are made. These four parameters have an effect on the quality of salami.

In Tunisia, the numerical modeling of the meat industry processes has not been studied. Therefore, validated computer models to simulate cooking and cooling of cooked meat products are needed. So, in order to simulate and optimize the cooking and cooling process for cooked meats, in the current study, a heat transfer model is developed. The main objective of this research is to define a model that describes heat transfer during cooking and cooling of Tunisian salami and to develop and solve model in proprietary software (MATLAB). The model will be validated under meat processing conditions and adapted to provide accurate simulations based on parameters that can be easily provided by a meat processor. Latest aim is to make the model available to the meat industry.

2. MATERIALS AND METHODS

2.1. Samples

Salami samples were realized at a Tunisian producer (SAVIMO, Boumhel Ben Arous, Tunisia). Salami was made from crushed (minced) meat and emulsified fats. Raw product is filled in a cylindrically shaped gut. Sample dimensions were 5.6 x 24 (diameter x length) and mean weight was 565 g ± 5 g.

2.2. Cooking and cooling treatments

The product has been cooked in steam oven with a volume of 2 x 1 x 1.5 = 3 m³ until at least 75°C core temperature was reached. Cooking time was 95 min. The steam allows an

excellent heat exchange with the product and ensures good homogeneity of temperature. For the study of the heat transfer and model validation, cooking and cooling trials were carried out in quadruplicate. The oven temperature was monitored with wire thermocouples (E-type; Ni/Al-Ni/Cu). After cooking, cooling is very important step to avoid microbial development. The cooling was carried out in two phases: immersion water and air cooling processes. The first one consists on pulverization of water at 19-20°C during 50 min. For the second step samples were treated with air at temperature of 2-4°C. Temperature data were collected in an Excel (Microsoft product) worksheet.

3. MODEL DEVELOPMENT

3.1. Heat transfer equation

In the cooked meat industry, meat joints are formed by small pieces of boned-out legs and the joints are injected with brine solution. Therefore there is abundance of macro-pores among the meat pieces. For developing the model, the cooked meat sample is assumed to be in a cylindrical shape (Fig. 1).

The heat transfer equation for the cooked meat is heat conduction in a homogeneous, isotropic body without inner heat generation. Initially, the temperature is evenly distributed in the product.

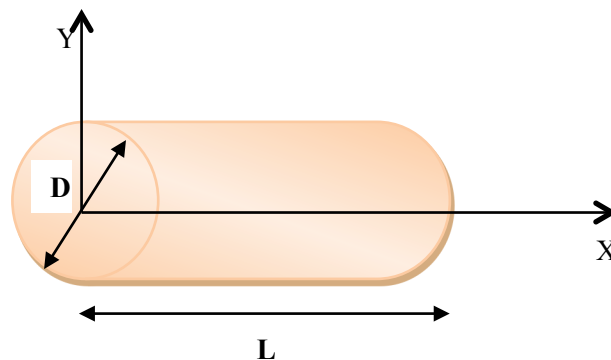


Figure 1. Shape of the cooked meat sample.

$$\rho \cdot Cp \cdot \frac{\partial T}{\partial t} = k \nabla^2 T \quad (1)$$

In a cylindrical coordinate system, the equation of the heat conduction can be written in the following form:

$$\rho \cdot Cp \cdot \frac{\partial T}{\partial t} = k \cdot \frac{1}{r} \cdot \frac{\partial}{\partial r} \left(r \cdot \frac{\partial T}{\partial r} \right) + \frac{\partial^2 T}{\partial z^2} \quad (2)$$

Or else:

$$\rho \cdot Cp \cdot \frac{\partial T}{\partial t} = k \cdot \frac{1}{r} \cdot \left(\frac{\partial T}{\partial r} + r \frac{\partial^2 T}{\partial r^2} \right) + \frac{\partial^2 T}{\partial z^2} \quad (3)$$

The initial condition is as follows: It is considered that the temperature distribution is uniform in the product:

$$t = 0, \quad T(r, t) = T(r, 0) = T_0 \quad (4)$$

$$t = 0, \quad T(z, t) = T(z, 0) = T_0 \quad (5)$$

The boundary conditions were: Product is maintained at the temperature of the oven during cooking and the temperature of cold room during cooling:

$$T(r, t) = T(z, t) = T_a \quad (6)$$

The physical characteristics of salami (CHEN *et al.*, 1999) are shown in the Table 1.

Table 1. Physical characteristics of salami.

Symbol	Definition	Value	Units
C_p	Heat capacity	3530	J/kg K
K	Thermal conductivity	0.412	W/m K
P	Density	1100	kg/m ³

3.2. Meshing and Discretization of differential equations

It performs a discretization of the domain validation of differential equations: the temperature should be calculated by a finite number of points. To simplify, the selected mesh is a grid of step:

$$\Delta r = \Delta z = p \text{ (Fig. 2).}$$

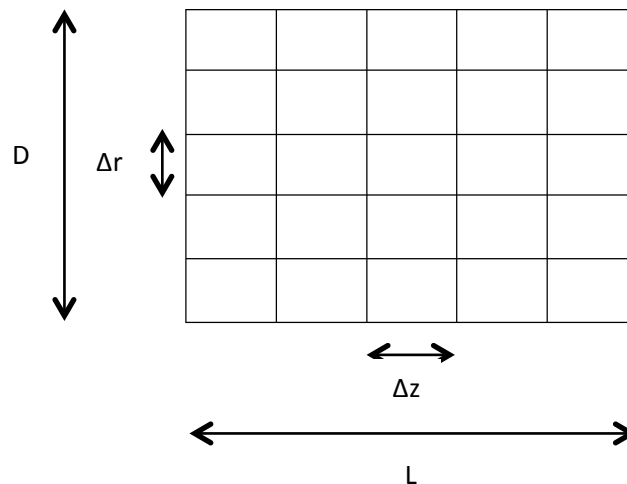


Figure 2. Domain mesh system.

In the system of validating domain of differential equations, any point M is located on a coordinate node (r_i, z_j, t_k) , with:

$$\begin{aligned} r_i &= i \times \Delta r; i \text{ between } 0 \text{ and } n, \\ z_j &= j \times \Delta z; j \text{ between } 0 \text{ and } m, \\ t_k &= k \times \Delta t; k \text{ between } 0 \text{ and } q. \end{aligned}$$

The finite difference approximations for derivatives are one of the simplest and of the oldest methods to solve differential equations. The advent of finite difference techniques in numerical applications began in the early 1950s and their development was stimulated by the emergence of computers that offered a convenient framework for dealing with complex problems of science and technology.

The principle of finite difference methods is close to the numerical schemes used to solve ordinary differential equations. It consists in approximating the differential operator by replacing the derivatives in the equation using differential quotients. The domain is partitioned in space and in time and approximations of the solution are computed at the space or time points. The error between the numerical solution and the exact solution is determined by the error that is committed by going from a differential operator to a difference operator.

The first derivative and the second derivative of the differential equation can be represented in different ways, in the form of finite difference, using the Taylor series development.

The approximation of $\frac{\partial T}{\partial t}$ is obtained by the Taylor expansion in the first order of the function $T(r, t)$.

$$\frac{\partial T}{\partial t} = \frac{T(r, t+dt) - T(r, t)}{dt} \quad (7)$$

The same for the approximation of $\frac{\partial T}{\partial r}$:

$$\frac{\partial T}{\partial r} = \frac{T(r+dr, t) - T(r, t)}{dr} \quad (8)$$

The approximation of $\frac{\partial^2 T}{\partial r^2}$ is obtained by the Taylor expansion in the second order:

$$T(r + dr, t) = T(r, t) + \frac{\partial T}{\partial r}(r, t)dr + \frac{1}{2} \frac{\partial^2 T}{\partial r^2}(r, t)dr^2 \quad (9)$$

$$T(r - dr, t) = T(r, t) - \frac{\partial T}{\partial r}(r, t)dr + \frac{1}{2} \frac{\partial^2 T}{\partial r^2}(r, t)dr^2 \quad (10)$$

$$T(r + dr, t) + T(r - dr, t) = 2T(r, t) + \frac{\partial^2 T}{\partial r^2}(r, t)dr^2 \quad (11)$$

$$\frac{\partial^2 T}{\partial r^2}(r, t) = \frac{T(r+dr, t) + T(r-dr, t) - 2T(r, t)}{dr^2} \quad (12)$$

And similarly for the approximation of $\frac{\partial^2 T}{\partial z^2}$, we obtain:

$$\frac{\partial^2 T}{\partial z^2}(z, t) = \frac{T(z+dz, t) + T(z-dz, t) - 2T(z, t)}{dz^2} \quad (13)$$

Hence, the differential equation (3) is approximated as follow:

$$\rho \cdot Cp \cdot \frac{\partial T}{\partial t} = k \cdot \frac{1}{r} \cdot \left(\frac{\partial T}{\partial r} + r \frac{\partial^2 T}{\partial r^2} \right) + \frac{\partial^2 T}{\partial z^2}$$

So:

$$\rho \cdot Cp \cdot \frac{T(r, t+dt) - T(r, t)}{dt} = k \cdot \frac{1}{r} \cdot \left(\frac{T(r+dr, t) - T(r, t)}{dr} + r \frac{T(r+dr, t) + T(r-dr, t) - 2T(r, t)}{dr^2} \right) + \frac{T(z+dz, t) + T(z-dz, t) - 2T(z, t)}{dz^2} \quad (14)$$

3.3. Evaluation of model performance

Model performance evaluation was carried out by comparing the deviation between the observed and predicted temperatures in different (r, z) locations over time. It was estimated by calculating the root mean square error (RMSE) per each validation test (Equation 15).

$$RMSE = \sqrt{\frac{\sum_{i=1}^n (T_{observed} - T_{predicted})^2}{n}} \quad (15)$$

Where n represents the number of observations.

The mean RMSE among the validation tests \pm standard deviation was used to report the overall performance model.

In addition, the assessment of the prediction accuracy of the numerical simulation was made by comparison of the numerically calculated temperature with the experimentally measured temperature. The percentage differences were calculated from (DELGADO and SUN, 2003):

$$Diff(\%) = \frac{Predicted\ temperature - Experimental\ temperature}{Experimental\ temperature} \times 100 \quad (16)$$

4. RESULTS AND DISCUSSIONS

4.1. Temperature distribution

During cooking, it is assumed that the initial temperature of the cooked meats is homogeneous. Initially, the temperature of the salami is 15°C and the oven temperature is

20°C. However, we measured the temperature after one hour (3600 s), since we cannot insert probe thermometer at the beginning of cooking as the initial state of salami is pasty. The results of the numerical solution of the discrete equation are shown in Fig. 3. We observe that as the heat flows by conduction described by the Fourier equation in our model, the interior temperature rises slowly at both heating ends. Also, we note that the temperature equilibrates in the interior of the salami as time proceeds.

It may be noted that this typical profile of the heat transfer will be obtained irrespective of a 1-D or 2-D approach, given the temperature profile is evaluated at the central axis of the salami. However, when considering the spatial temperature profile, the edges of the salami sample are open to the ambient environment, which causes a heat loss. This is in agreement with the experimental results reported by CHAPWANYA and MISRA (2015).

Finally, we also observe from Fig. 3 that the temperature at the core/geometric center of the salami of diameter 5.6 cm reaches a temperature of 59.41°C in 60 min. Then, the temperature continues to rise, reaching 75.21°C after 35 min of heating. Conduction heating of salami involves the transfer of kinetic energy between non-isothermal adjacent layers, without mass transfer. TOM *et al.* (2013) employed Kelvin equation and Halsey equation to determine the average pore size of beef. The authors report that the pores enlarge with increase in moisture levels and sorption temperature. It should be noted that the porosity refers to volume fraction of solvent. We can suppose, in our case, that the porosity of artificial gut and moisture follow this relation and also support the observations made by TOM *et al.* (2013).

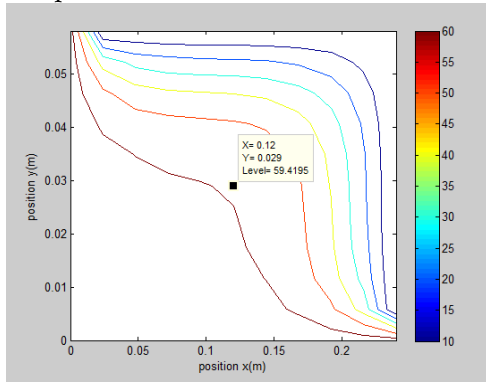
RINALDI *et al.* (2011) studied simultaneous heat and mass transfer for cooking process of Mortadella Bologna PGI. The authors developed mathematical model to estimate thermal and mass properties by means of direct finite differences method. Weight loss was significantly lower at 80°C (4.56%) in comparison with those obtained at 90 and 100°C (5.46 and 5.44%), while no significant differences were found between the latter. Water content decreased at the surface and half-radius of the samples as oven temperature increased, as expected, due to the evaporation. In contrast, water content did not show significant differences at Mortadella center among the three temperatures (80, 90 and 100°C), probably due to the low water diffusion rate within this section. This aspect didn't carry out in our work. It may be studied in the future. Thermal processing involves not only simultaneous heat and mass transfer, but also physicochemical reactions, such as protein denaturation. The thermal properties of salami change during processing.

Temperature distributions for cooling process (water immersion) are shown in Fig. 4. We also observe from that the temperature at the core/geometric center of the salami is 5.6 cm in diameter reaches a 30.58°C in 50 min of cooling. Predicted temperature distributions for cooling process (air) are shown in Fig. 5. We also observe from that the temperature at the core/geometric center of the salami is 5.6 cm in diameter reaches a 10.45°C in 40 min of cooling. For the two cooling phases, cooling time to reach 10.45°C at the salami center was 90 min.

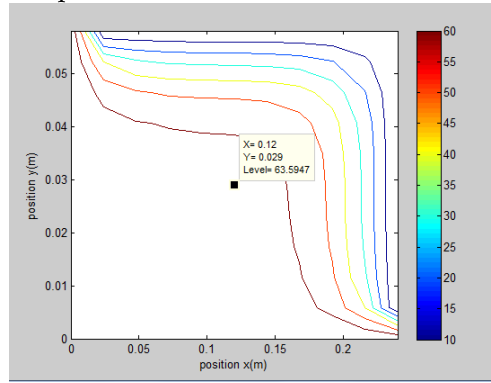
An integrated model of heat transfer and dynamic growth of *C. perfringens* in cured salami was developed and validated for three cooling scenarios (AMÉZQUITA *et al.*, 2005). Results showed good agreement between predicted and experimental data. So, effective integration of engineering and microbial modeling offer a useful quantitative tool to support several food safety and microbiological risk assessment.

In a first time, the agreement between the predicted and the experimental kinetics allows us to validate the model hypothesis and has ensured us a quite good accuracy even if we are aware of the fact that this model is quite simplified in the heat transfer on a homogeneous and isotropic medium. In a second time, to face this challenge and improve the efficiency of our model, the next steps of this work will be to implement the composition of salami and its various ingredients.

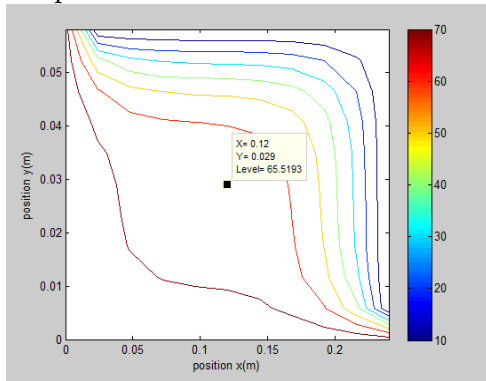
Temperature distribution for t = 3600 s



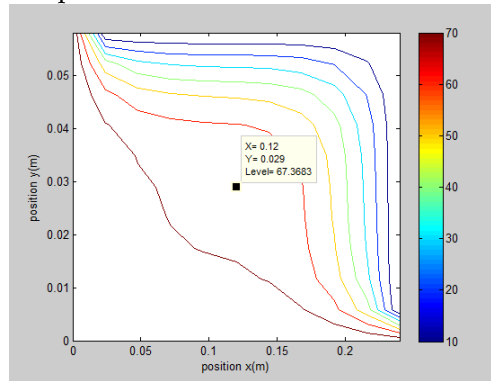
Temperature distribution for t = 3900 s



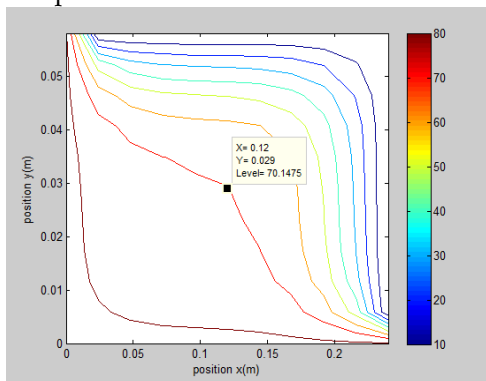
Temperature distribution for t = 4200 s



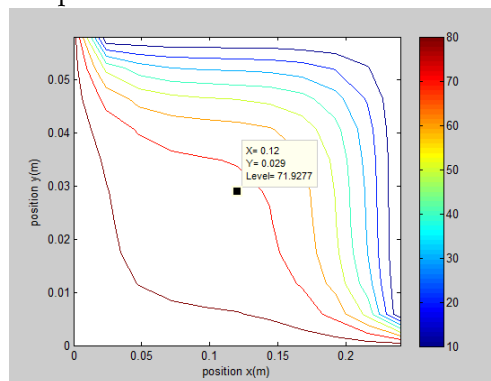
Temperature distribution for t = 4500 s



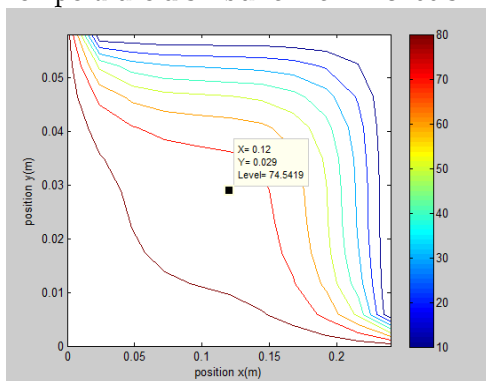
Temperature distribution for t = 4800 s



Temperature distribution for t = 5100 s



Temperature distribution for t = 5400 s



Temperature distribution for t = 5700 s

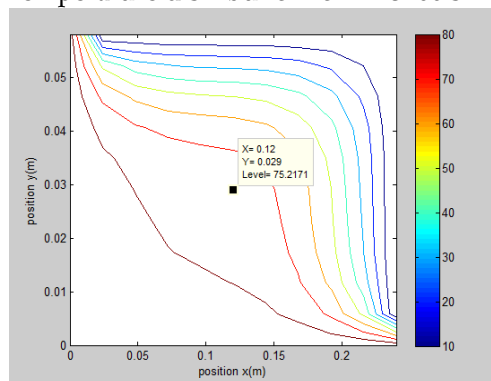
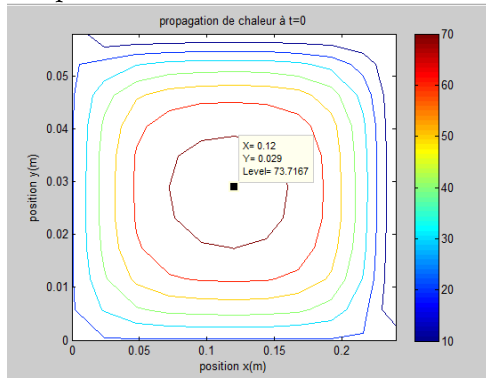
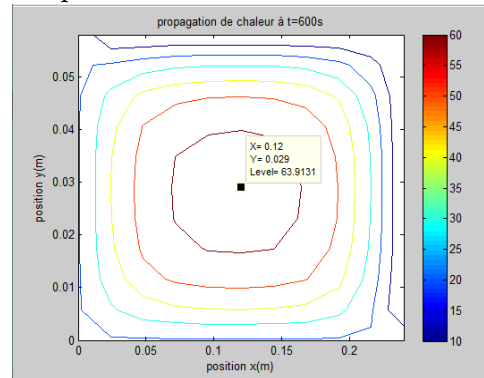


Figure 3. Predicted temperature ($^{\circ}\text{C}$) distributions for cooking process.

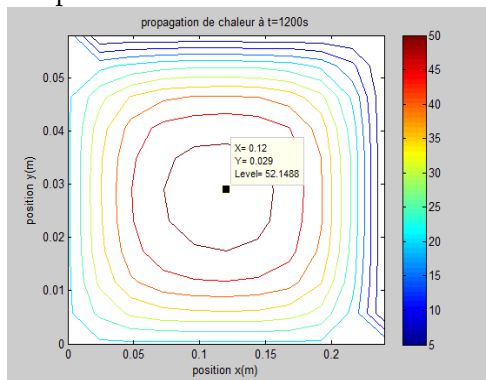
Temperature distribution for t = 0 s



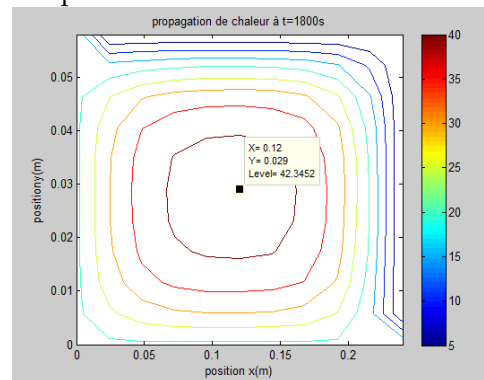
Temperature distribution for t = 600 s



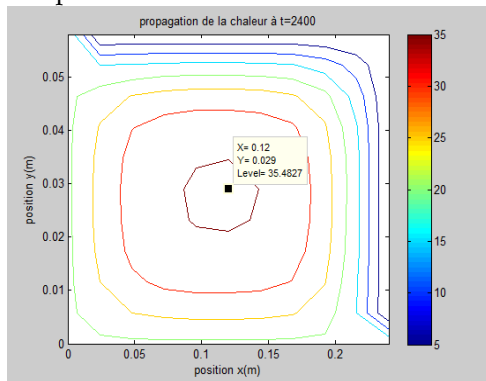
Temperature distribution for t = 1200 s



Temperature distribution for t = 1800 s



Temperature distribution for t = 2400 s



Temperature distribution for t = 3000 s

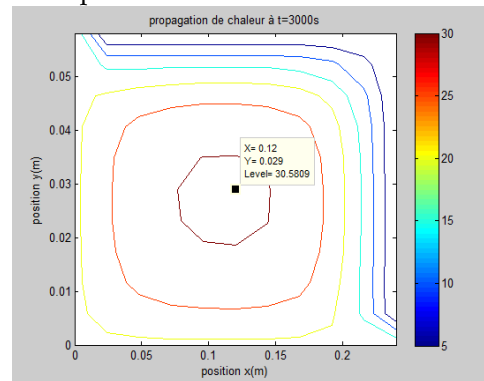
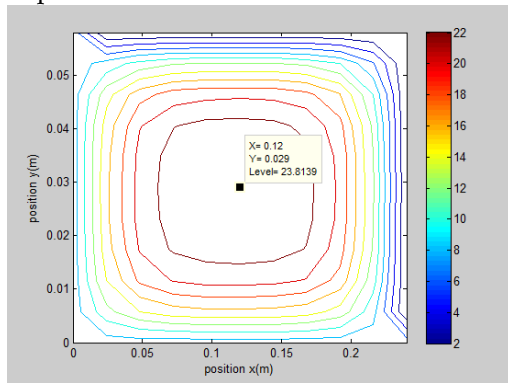
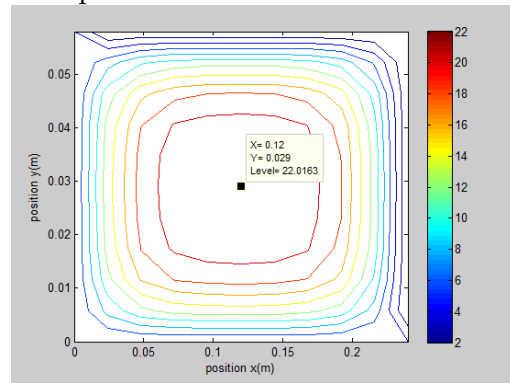


Figure 4. Predicted temperature ($^{\circ}\text{C}$) distributions for cooling process (water immersion).

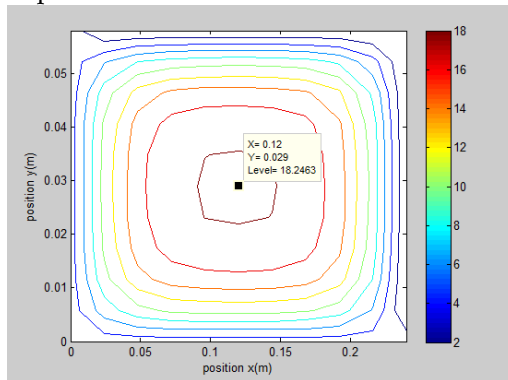
Temperature distribution for $t = 0+3000$ s



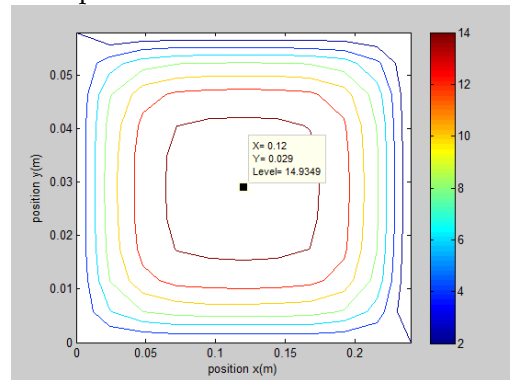
Temperature distribution for $t = 600+3000$ s



Temperature distribution for $t = 1200+3000$ s



Temperature distribution for $t = 1800+3000$ s



Temperature distribution for $t = 2400+3000$ s

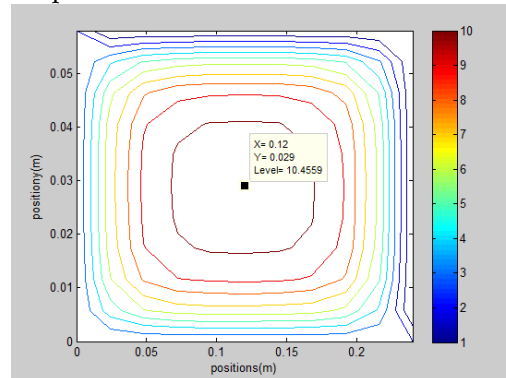


Figure 5. Predicted temperature ($^{\circ}\text{C}$) distributions for cooling process (air).

The heat released from the product surface to the cooling medium (water) by convection, depends on its properties and parameters, such as its viscosity, density, turbulence and so on, as well as on surface roughness and on the geometry of the salami. Comparing the two cooling processes, we note that the kinetics of the process using water immersion ($0.87\text{ }^{\circ}\text{C} / \text{min}$) is faster than that of the cooling air process ($0.33\text{ }^{\circ}\text{C} / \text{min}$). Ayadi and colleagues (2009) shows that the variation of the heat penetration is attributed to raw material and formulation. Material composition affects the hardness and the elasticity of cooked meat during heating. Thus, textural and sensorial characteristics of salami change.

In previous work, mathematical modelling of heat transfer in Mortadella Bologna PGI during evaporative pre-cooling was studied (RINALDI *et al.*, 2014). Mortadella evaporative pre-cooling process from 70 to 50°C at core was investigated. The effects of ventilation and water spraying with different intervals (0, 5, 10 and 15 min) were tested at core and surface temperatures and cooling times were compared. Both ventilation and water spraying increased the cooling rate.

The slowest and the fastest cooling rates were obtained under no ventilation and no water spraying condition, and with ventilation and water spraying every 5min, respectively. In this last condition, about half time was required to reach 50 °C at the product thermal core compared to first one sample. Compared to these results we can conclude that two phases cooling processes (immersion water + air) is the fastest than the combined one (ventilation + spraying).

4.2. Model performance

In order to validate the model, we set-up the parameters for numerical simulations as per those of experiments. Fig. 6 presents the evolution of both experimental and simulated salami temperature profiles. Firstly, we observe that the temperature of the geometric center of the salami shows a continuous increase and decrease respectively for cooking and cooling processes.

To evaluate the accuracy of the models, we employ the statistical criterion of the Root Mean Squared Error (RMSE). The proposed model was in good agreement with the experimental values when the simulations were carried out including initial conditions, boundary conditions and physical characteristics of salami. However, the best prediction was obtained when both thermal conductivity and specific heat were modeled as state-dependent functions in the simulation (CHEN *et al.*, 1999).

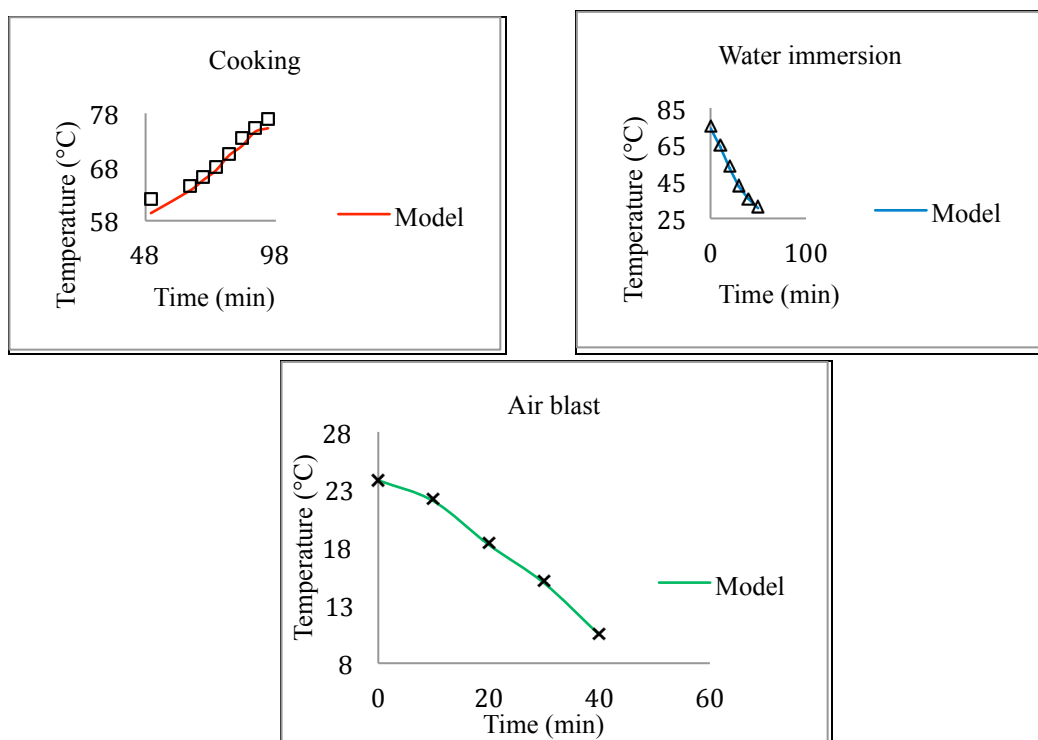


Figure 6. Evolution of experimental (open symbols) and simulated temperature (solid line) at the core of salami.

Calculated RMSE and percentage differences values were presented in Table 2.

Table 2. Evaluation of model performance at core of product.

Processes	RMSE (°C)	Diff (%)
Cooking	1.09 ± 0.72	1.58
Cooling (water immersion)	0.87 ± 0.45	1.72
Cooling (air blast)	0.116 ± 0.087	0.66

In theory, the accuracy of the predictions can be improved when a method for getting better estimations of initial temperatures within the product prior to cooling, and temperature distribution of the air surrounding the products are available. This difference could be due to several reasons (PAN *et al.*, 2000). The primary cause for this difference may be the slight dislocation of the thermocouple junction, placed initially at the center of the salami. Although the thermocouple location was verified at the end of the experiment, the non-rigid state of the cooked salami may result in some movement of the thermocouple. The thermal properties were estimated for use in the model. A certain level of uncertainty in predicted values is due to the estimated values of properties. Regardless of these uncertainties, the predicted values are in good agreement with the experimental data as seen in Figure 6. Future research is needed to determine the variation of thermal properties with temperature for salami cooking.

In previous work, transient temperature distributions inside the chicken patties were predicted (CHEN *et al.*, 1999). Samples were cooked in a convection oven for model validation. The predicted transient center temperature had an error of 3.8 ± 5.7 °C, as compared to experimental data. However, the best prediction was obtained when both thermal conductivity and specific heat were modeled as state-dependent functions in the simulation (CHEN *et al.*, 1999).

A similar approach was applied for simulation and experimental validation of simultaneous heat and mass transfer for cooking process of Mortadella Bologna PGI (RINALDI *et al.*, 2011). Obtained errors (RMSE) were higher compared to this work. This result is confirmed by RINALDI *et al.* (2014), it is probably due to both phenomena summed together by coupling mass end heat transfer.

5. CONCLUSIONS

The cooking and cooling processes of Tunisian salami (cooked meat) are modeled. Two cooling processes are carried out: cooling air blast and cooling water immersion. The finite difference numerical method is used to solve the model. The model demonstrated good predictive capabilities for core temperature of the salami. The model has some issues in predicting temperatures for some hams that needs to be addressed (type of gut, composition, formulation).

The mathematical method developed has successfully described the temperature evolution in the salami. Experimentally measured and calculated results are in good agreement, especially during the first (water immersion) and second (air blast) stages of cooling. The maximum deviation between measured and calculated temperatures was within 2.59°C for the cooking, within 1.49°C for the cooling by immersion water and within 0.19°C for the air blast cooling processes. Percentage differences between predicted

and experimental temperatures for the cooking, cooling by immersion water and air blast cooling processes were around 1.58%, 1.72% and 0.66%, respectively.

Although we considered the case of salami heating to demonstrate the validity of the model, the modification of boundary conditions for other cases heating with flipping, oven roasting or frying should be straightforward. The opening of the oven while cooking the salami may be incorporated with appropriate functional relationship of the temperature determined experimentally with time. Furthermore, with incorporation of equations for microbial inactivation, this model could also be used to predict microbial safety.

ACKNOWLEDGEMENTS

Author gratefully acknowledges Mr Sahbi BOUAZIZI (English teacher at Ecole Supérieure des Ingénieurs de l'Équipement Rural, ESIER, Medjez el Bab, Tunisia) for reviewing the English of this paper.

NOMENCLATURE

ρ	Density (kg/m ³)
C_p	Heat capacity (J/kg K)
k	Thermal conductivity (W/m K)
T	Temperature (°C)
t	Time (s)
∇	Divergency operator
r	Radius (m)
D	Diameter (m)
L	Length (m)

REFERENCES

- Amézquita A., Weller C.L., Wang L., Thippareddi H. and Burson D.E. 2005. Development of an integrated model for heat transfer and dynamic growth of *Clostridium perfringens* during the cooling of cooked boneless ham. *International Journal of Food Microbiology* 101:123-144.
- Ayadi M.A., Makni I. and Attia H. 2009. Thermal diffusivities and influence of cooking time on textural, microbiological and sensory characteristics of turkey meat prepared products. *Food and Bioproducts Processing* 87:327-333.
- Cepeda J.F., Weller C.L., Thippareddi H., Negahban M. and Subbiah J. 2013. Modeling cooling of ready-to-eat meats by 3D finite element analysis: Validation in meat processing facilities. *Journal of Food Engineering* 116:450-461.
- Chapwanya M. and Misra N.N. 2015. A mathematical model of meat cooking based on polymer-solvent analogy. *Applied Mathematical Modelling* 39:4033-4043.
- Chen H., Marks B.P. and Murphy R.Y. 1999. Modeling coupled heat and mass transfer for convection cooking of chicken patties. *Journal of Food Engineering* 42:139 - 146.
- Cogné C., Nguyen, P.U., Lanoisellé J.L., Van Hecke E. and Clausse D. 2013. Modeling heat and mass transfer during vacuum freezing of puree droplet. *International Journal of Refrigeration* 36:1319-1326.
- Delgado A.E. and Sun D.W. 2003. One-dimensional finite difference modeling of heat and mass transfer during thawing of cooked cured meat. *Journal of Food Engineering* 57:383-389.
- Drummond L. and Sun D.W. 2008. Temperature evolution and mass losses during immersion vacuum cooling of cooked beef joints – A finite difference model. *Meat Science* 80:885-891.
- Holm E.S, Adamsen A.P.S., Feilberg A., Schäfer A., Løkke M.M. and Petersen M.A. 2013. Quality changes during storage of cooked and sliced meat products measured with PTR-MS and HS-GC-MS. *Meat Science* 95:302-310.
- Hu Z. and Sun D.W. 2000. CFD simulation of heat and moisture transfer for predicting cooling rate and weight loss of cooked ham during air-blast chilling process. *Journal of Food Engineering* 46:189-197.

- Kondjoyan A., Oillic S., Portanguen S. and Gros J.B. 2013. Combined heat transfer and kinetic models to predict cooking loss during heat treatment of beef meat. *Meat Science* 95:336-344.
- Pan Z., Singh R.P. and Rumsey T.R. 2000. Predictive modeling of contact-heating process for cooking a hamburger patty. *Journal of Food Engineering*, 46:9-19.
- Rinaldi M., Chiavaro E., Gozzi E. and Massini R. 2011. Simulation and experimental validation of simultaneous heat and mass transfer for cooking process of Mortadella Bologna PGI. *International Journal of Food Science and Technology* 46:586-593.
- Rinaldi M., Chiavar, E. and Massini R. 2014. Mathematical Modelling of Heat Transfer in Mortadella Bologna PGI during Evaporative Pre-Cooling. *International Journal of Food Engineering* 10:233-241.
- Sun D.W. and Wang L. 2006. Development of a mathematical model for vacuum cooling of cooked meats. *Journal of Food Engineerin*, 77 379-385.
- Tom A., Bruneau D., Alexis K. and Aregba A.W. 2013. Desorption isotherms for fresh beef: an experimental and modeling approach. *Meat Science*, 96:1417-1424.
- Wang L. and Sun D.W. 2002. Evaluation of performance of slow air, air blast and water immersion cooling methods in the cooked meat industry by the finite element method. *Journal of Food Engineering*, 51:329-340.
- Wang L. and Sun D.W. 2004. Effect of operating conditions of a vacuum cooler on cooling performance for large cooked meat joints. *Journal of Food Engineering*, 61:231-240.

Paper Received November 5, 2016 Accepted June 25, 2017